H-bond itself ($\Delta G_{H\text{-}bond}$) is significantly higher than the observed ΔG of 4.0 kcal/mol.

The "intrinsic binding energy" of the amide N–H in **1** is considerably greater than the values reported by Fersht *et al.* (*9*) as representative of hydrogen bonds between uncharged components in the active site of tyrosyl-tRNA synthetase. Although a formal charge does not reside on the nitrogen, it may be argued that the phosphonamidate is not an uncharged species. However, the hydrogen bond formed between the phosphonamidate-NH and the active site hydrogen bond acceptor must be a highly favorable one from the point of view of entropy: both components are held in the same orientation in the absence of the interaction, hence no further entropy is lost on establishment of the hydrogen bond. This system therefore comes closest to approximating the situation envisaged by Jencks for determination of a true intrinsic binding energy (*2*). Were the interaction between flexible side chains, or between groups that are free to rotate before the hydrogen bond is established, a less favorable incremental binding energy would be seen. Thus, the value observed for a hydrogen bonding interaction may reflect the degree with which the interacting components are fixed as much as it does their charged or uncharged nature.

REFERENCES AND NOTES

1. W. P. Jencks, *Adv. Enzymol.* **43**, 219 (1975); A. Fersht, *Enzyme Structure and Mechanism* (Freeman, New York, ed. 2, 1985).
2. W. P. Jencks, *Proc. Natl. Acad. Sci. U.S.A.* **78**, 4046 (1981).
3. P. A. Bartlett and C. K. Marlowe, *Biochemistry* **22**, 4618 (1983).
4. R. Wolfenden, *Annu. Rev. Biophys. Bioeng.* **5**, 271 (1976).
5. The phosphonate esters were synthesized by coupling the phosphonochloridate, **i**, with the appropriate hydroxyamide, **ii**, and then cleaving the ester with lithium *n*-propyl mercaptide in HMPA [P. A. Bartlett and W. S. Johnson, *Tetrahedron Lett.* **1970**, 4459 (1970)]. The diacids were purified by ion exchange chromatography and isolated as crystalline solids that were characterized by ^{1}H, ^{13}C, and ^{31}P NMR spectroscopy and combustion analysis. Full details for the synthesis and characterization of the phosphonate ester inhibitors and for the enzymatic assays can be obtained from P. A. Bartlett.

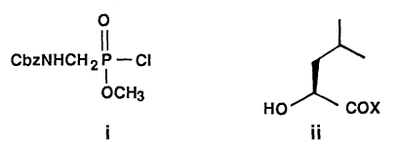

i ii

6. D. E. Tronrud, H. M. Holden, B. W. Matthews, *Science* **235**, 571 (1987).
7. L. H. Weaver, W. R. Kester, B. W. Matthews, *J. Mol. Biol.* **114**, 119 (1977).
8. J. Hine, *J. Am. Chem. Soc.* **94**, 5766 (1972).
9. A. R. Fersht *et al.*, *Nature (London)* **314**, 235 (1985).
10. T. A. Mastryukova and M. I. Kabachnick, *Russ. Chem. Rev.* **38**, 795 (1969); *J. Org. Chem.* **36**, 1201 (1971); M. Charton, *ibid.* **34**, 1877 (1969). The pK_a for methyl *N*-methylphosphoramidate, for example, is 2.50 [I. Oney and M. Caplow, *J. Am. Chem. Soc.* **89**, 6972 (1967)], whereas that for dimethyl phosphate is 1.29 [W. D. Kumler and J. J. Eiler, *ibid.* **65**, 2355 (1943)].
11. M. Wozniak and G. Nowogrocki, *Talanta* **26**, 381 (1979).
12. R. Wolfenden and R. Williams, *J. Am. Chem. Soc.* **105**, 1028 (1983).
13. P. A. Bash, U. C. Singh, F. K. Brown, R. L. Langridge, P. A. Kollman, *Science* **235**, 574 (1987).
14. P. J. F. Henderson, *Biochem J.* **127**, 312 (1972); I. M. Segel, *Enzyme Kinetics* (Wiley, New York, 1975), p. 158.

15. We thank B. W. Matthews, P. A. Bash, P. A. Kollman, and T. Alber for discussions, suggestions, and sharing information. This research was supported by NIH grant CA-22747.

22 August 1986; accepted 4 December 1986

Structures of Two Thermolysin-Inhibitor Complexes That Differ by a Single Hydrogen Bond

DALE E. TRONRUD, HAZEL M. HOLDEN,* BRIAN W. MATTHEWS†

The mode of binding to thermolysin of the ester analog Cbz-Gly^{P}-(O)-Leu-Leu has been determined by x-ray crystallography and shown to be virtually identical (maximum difference 0.2 angstrom) with the corresponding peptide analog Cbz-Gly^{P}-(NH)-Leu-Leu. The two inhibitors provide a matched pair of enzyme-inhibitor complexes that differ by 4.1 kilocalories per mole in intrinsic binding energy but are essentially identical except for the presence or absence of a specific hydrogen bond.

CRYSTALLOGRAPHIC ANALYSES OF the thermostable endopeptidase thermolysin have revealed the modes of binding of a broad spectrum of inhibitors (*1–5*) and have led to a detailed proposal for the stereochemical mechanism of action of the enzyme (*6*). In brief, Glu 143, in concert with the zinc, is presumed to promote the attack of a water molecule on the carbonyl carbon of the scissile bond. The proton accepted by Glu 143 is then shuttled to the leaving nitrogen. An analogous mechanism was also proposed for carboxypeptidase A (*5*) and is supported by the recent finding that Tyr 248 of carboxypeptidase A is not required for catalysis (*7*).

Here we describe the mode of binding to thermolysin of Cbz-Gly^{P}-(O)-Leu-Leu [hereafter ZG^{P}(O)LL], one of a series of phosphorus-containing inhibitors of thermolysin (*4, 8–10*) developed by Bartlett and Marlowe (*10, 11*) as putative transition-state analogs of ester substrates. [As in the preceding report (*11*) the superscript P indicates that the inhibitor has a tetrahedral phosphonamide or phosphonate ester linkage.] We found that the mode of binding of this ester analog is very similar to the corresponding peptide analog Cbz-Gly^{P}-(NH)-Leu-Leu (hereafter ZG^{P}LL). This allows the difference in affinity of the two inhibitors for thermolysin to be ascribed directly to differences in solvation and hydrogen

Institute of Molecular Biology, University of Oregon, Eugene, OR 97403.

*Present address: Department of Biochemistry, Biological Sciences West, University of Arizona, Tucson, AZ 85721.

†To whom correspondence should be addressed.

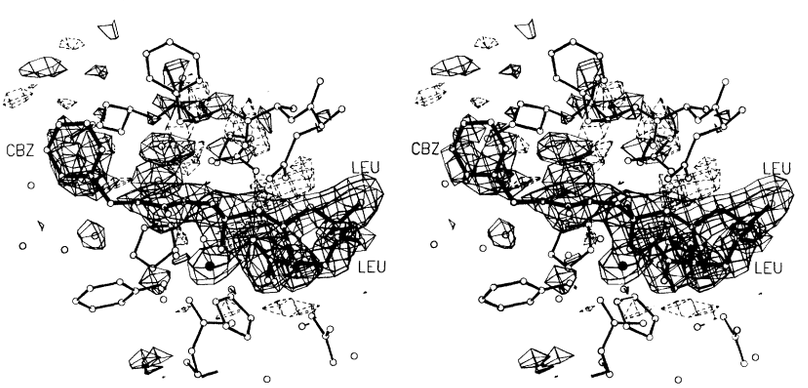

Fig. 1. Difference electron density for ZG^{P}(O)LL bound to crystalline thermolysin. Coefficients for the map are of the form ($F_{complex} - F_{native}$) where the native amplitudes and phases are calculated for the refined structure with active-site solvent atoms removed. Resolution 1.9 Å. Contours are drawn at height $+2\sigma$ (solid) and -2σ (broken) where σ is the root-mean-square density throughout the unit cell. The difference electron density at the phosphorus position is 16σ. The bound inhibitor is drawn with bonds thicker than the protein. The zinc ion is drawn solid.

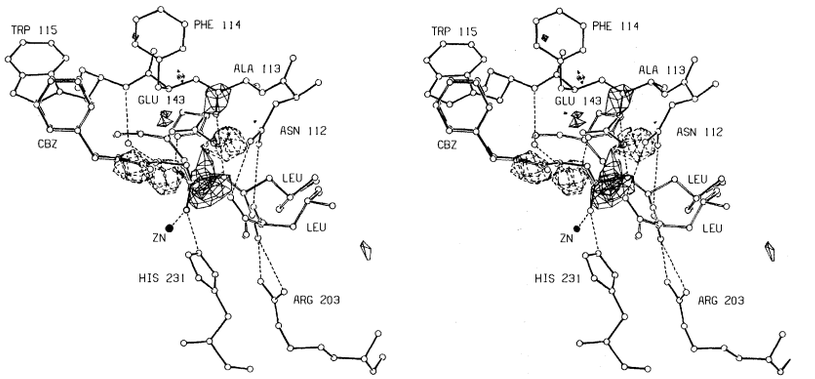

Fig. 2. Stereoscopic view of $ZG^P(O)LL$ bound in the extended thermolysin active-site cleft. Presumed hydrogen bonds are drawn as broken lines; ligands to the zinc are shown as dotted lines.

bonding of the free and bound ester and amide moieties.

One crystal of thermolysin soaked for 5 days in 1.0 m*M* $ZG^P(O)LL$, 10 m*M* calcium acetate, 10 m*M* tris, 7% DMSO (v/v), *p*H 7.2, sufficed for us to collect three-dimensional data to 1.6 Å resolution by methods previously described (*5, 12*). A total of 74,766 reflections were measured and reduced to 32,538 unique intensities with an average agreement of 4.3% between repeated measurements. The configuration of the bound inhibitor was initially visualized by using difference electron density maps (Fig. 1) and was refined by using the restrained least-squares refinement program TNT (*9, 13*) to a crystallographic residual of 17.1% at 1.6 Å resolution. The root-mean-square deviation from "ideal" geometry is 0.023 Å for bond lengths, 3.8° for bond angles, and 0.02 Å for groups of atoms expected to be coplanar. The structure of the complex of thermolysin with the peptide analog ZG^PLL has also been determined and refined crystallographically under similar conditions (*14*).

$ZG^P(O)LL$ is the first analog of an ester substrate at thermolysin to be examined crystallographically. Its mode of binding is shown in Fig. 2. As expected, the phosphonate group forms a ligand to the zinc (Fig. 3) and the adjacent leucyl side chain occupies the S_1' specificity pocket. The bound complex of $ZG^P(O)LL$ is practically superimposable on its amide counterpart (Table 1 and Figs. 3 and 4). Very small changes in the free enzyme structure (at most a few tenths of an angstrom) occur on binding either the ester or the peptide analog. These results are consistent with the hypothesis that thermolysin-catalyzed hydrolysis of peptides and esters proceeds by a similar mechanism.

Although the configurations adopted by $ZG^P(O)LL$ and ZG^PLL are very similar, there are some small but significant differences in the coordinates of the respective enzyme-inhibitor complexes. To show that these differences are real, we show in Fig. 5 the difference in electron density between the two inhibitor complexes. The map has significant positive and negative peaks ($\pm 6\sigma$), indicating that the small differences of 0.12 Å in the phosphorus position and 0.21 Å in the oxygen atoms OP2 of the two bound inhibitors (Table 1) are significant. The difference map (Fig. 5) also indicates that there is a significant shift (about 0.35 Å) in the position occupied by the carboxyl group of Glu 143. This is of particular interest since Glu 143 is thought to be the critical residue in catalysis (*5, 6*). Why this

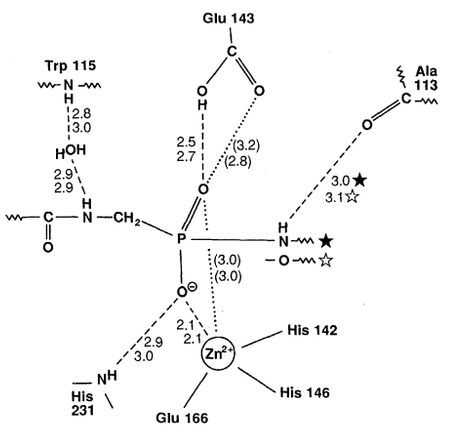

Fig. 3. Schematic drawing comparing enzyme-inhibitor interactions for $ZG^P(NH)LL$ (distances above) and $ZG^P(O)LL$ (distances underneath). Presumed hydrogen bonds are drawn as broken lines and other close approaches are shown dotted. The critical differences between the two inhibitors are emphasized by the solid stars (hydrogen bond present) and open stars (no hydrogen bond).

Table 1. Coordinates for Cbz-Gly^P-(O)-Leu-Leu. *X,Y,Z* are in the standard orthogonal thermolysin coordinate system [for example, see (*1*)]. *B* is the thermal parameter. Δr is the distance between corresponding atoms in ZG^PLL and $ZG^P(O)LL$ and ΔB is the difference between the thermal parameters ($ZG^PLL - ZG^P(O)LL$). The estimated uncertainty (*16, 17*) in the coordinates is 0.15 Å for the well-defined atoms ($B \leq 20$ Å^2); atoms with larger thermal factors are determined less reliably.

Group	Atom	*X* (Å)	*Y* (Å)	*Z* (Å)	*B* (Å^2)	Δr (Å)	ΔB (Å^2)
Cbz	OA	49.4	18.8	−9.8	30.0	0.12	−1.9
	CB	48.8	18.3	−11.1	30.5	0.14	−0.5
	CG	47.5	19.1	−11.5	25.8	0.13	0.1
	CD1	46.4	19.1	−10.6	26.7	0.16	−0.1
	CE1	45.1	19.6	−10.9	29.6	0.14	−4.7
	CZ	45.0	20.4	−12.0	22.1	0.12	1.2
	CE2	46.1	20.5	−12.8	25.7	0.18	0.9
	CD2	47.3	19.9	−12.6	30.0	0.15	−0.5
	C	49.7	17.9	−8.8	25.7	0.11	−4.7
	O	49.6	16.7	−9.0	20.5	0.03	0.0
Gly^P	N	50.1	18.6	−7.7	13.1	0.15	−2.5
	CA	50.4	17.9	−6.6	6.8	0.14	−3.0
	P	51.8	18.9	−6.0	11.3	0.12	−1.6
	OP1	53.0	18.7	−6.6	9.7	0.06	0.1
	OP2	51.6	20.5	−5.9	11.4	0.21	−0.8
(O)-Leu	ON	51.8	18.4	−4.5	5.0	0.13	−2.4
	CA	52.9	18.3	−3.6	11.6	0.07	1.7
	CB	52.5	18.3	−2.1	6.4	0.03	−0.9
	CG	53.7	18.1	−1.2	9.9	0.08	1.6
	CD1	54.6	19.4	−1.3	13.1	0.12	−2.5
	CD2	53.0	18.1	0.2	7.9	0.19	−0.2
	C	53.6	16.9	−3.9	18.6	0.07	1.3
	O	54.8	16.8	−3.8	10.6	0.05	−1.4
Leu	N	52.7	15.9	−4.1	11.0	0.06	0.7
	CA	53.1	14.5	−4.4	21.7	0.10	−1.4
	CB	53.5	13.7	−3.1	13.1	0.04	−1.4
	CG	52.3	13.5	−2.2	17.1	0.05	0.7
	CD1	52.4	14.5	−1.2	26.3	0.18	−2.7
	CD2	52.3	12.2	−1.5	24.2	0.04	0.5
	C	52.4	13.8	−5.5	21.8	0.01	0.2
	O	51.3	14.3	−5.9	13.2	0.04	−1.8
	OH	52.8	12.8	−6.1	21.3	0.07	−2.5

Fig. 4. The complex between thermolysin (red skeleton) and ZG^PLL (also red) is contrasted with that of the enzyme (blue) with $ZG^P(O)LL$ (green). The magenta and yellow lines correspond to overlapping regions of the two enzymes and inhibitors, respectively. The blue dots represent the solvent-accessible surface of the active site, and the magenta sphere the van der Waals surface of the zinc cofactor. The yellow dotted line illustrates the hydrogen bond between ZG^PLL and the carbonyl oxygen of Ala 113 (*18*).

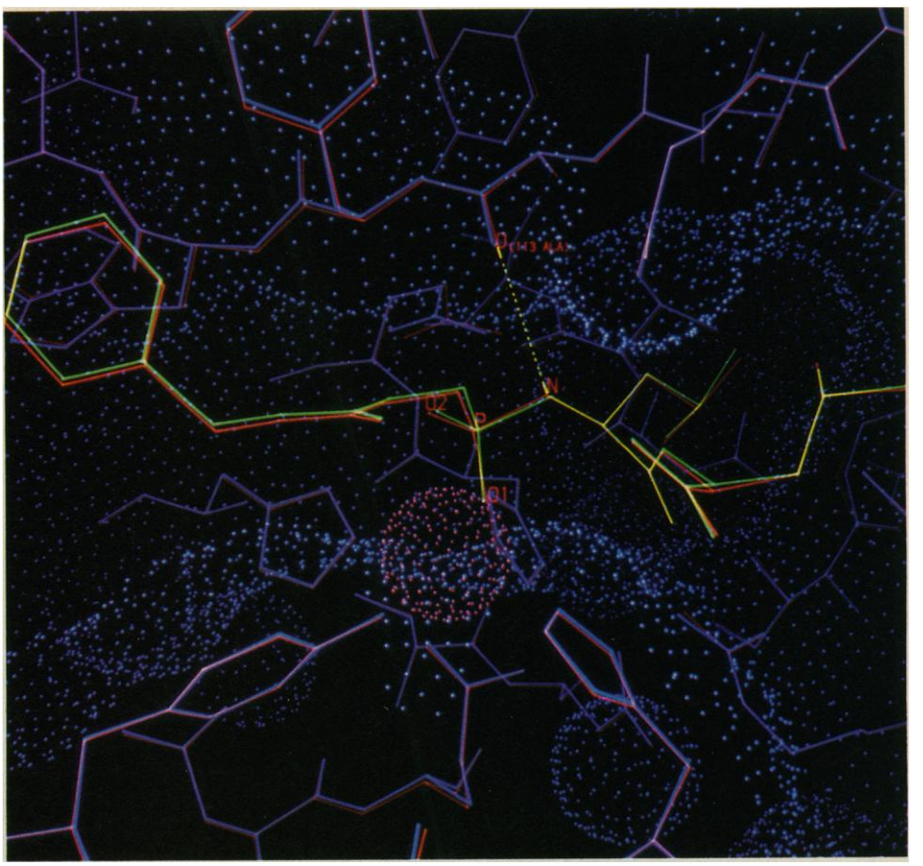

difference occurs in the respective inhibitor complexes is not obvious, especially since the movement of the carboxyl group does not alter its distance (3.4 Å) from the nitrogen/oxygen substitution site. Presumably the exact position occupied by the side chain of Glu 143 is sensitive to the overall charge distribution within the phosphonamide or phosphonate ester moieties. Such sensitivity, coupled with the ability to move, is consistent with the presumed role of Glu 143 as a proton shuttle during catalysis (*5, 6*).

Of particular interest in comparing the binding of $ZG^P(O)LL$ and ZG^PLL are any differences associated with the substitution of the –NH– by the ester oxygen. As can be seen in Figs. 2 to 4, when the –NH– is present a hydrogen bond (3.0 Å) is formed to the peptide carbonyl oxygen of Ala 113. Such a hydrogen bond has been seen previously with many thermolysin inhibitors and is presumed to occur in the transition state. When the –NH– is replaced by the ester oxygen, the corresponding enzyme-inhibitor distance remains virtually the same (3.1 Å) although no hydrogen bond can occur in this case. The lack of this hydrogen bond is one obvious factor that contributes to the different binding energy of $ZG^P(O)LL$ relative to ZG^PLL. Another factor to consider is a potentially unfavorable contact between the ester oxygen of $ZG^P(O)LL$ and the carbonyl oxygen of Ala 113 (Fig. 3). The observed oxygen-oxygen distance of 3.1 Å does not suggest an unfavorable contact, although the limited accuracy of the coordinates precludes a definitive statement. One also needs to consider the possibility of electrostatic effects due to differences in protonation when the respective inhibitors are bound or in solution. Because the expected pK_a of a glutamate (about 4.5) is 2 to 3 units higher than that of a phosphonamidate or a phosphonate ester (*8, 11*) it can be assumed that Glu 143, which is shielded from bulk solvent when both $ZG^P(O)LL$ and ZG^PLL are bound, is protonated at *p*H 7.2 and the $-PO_2-$ groups of each inhibitor carry a single negative charge (Fig. 3). The relatively short P–N bond length in ZG^PLL (1.66 Å) does not support the possibility that the nitrogen might be doubly protonated (cationic) or that the phosphonamide moiety might exist in a zwitterionic form. There could also be differential entropic effects, although, at least as indicated by their similar crystallographic thermal factors (Table 1), the respective enzyme-inhibitor complexes have comparable dynamics. As discussed in the accompanying reports (*11, 15*), the overall difference in binding energy of $ZG^P(O)LL$ and ZG^PLL derives not only from the respective enzyme-inhibitor complexes but also from differences in the energies of solvation of the free inhibitors.

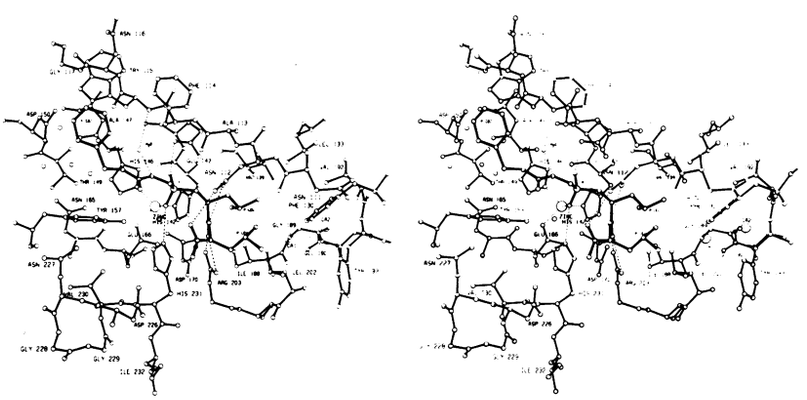

Fig. 5. Superposition of the refined structure of ZG^PLL (open bonds) on the refined $ZG^P(O)LL$–enzyme complex (solid bonds). Also shown is the position of Glu 143 (open bonds) in the ZG^PLL complex. The overlaid electron density contours show the difference in density between the two enzyme-inhibitor complexes. Coefficients are $(F_{ZG^P(O)LL} - F_{ZG^PLL})$ and phases for native thermolysin. Resolution 1.9 Å. Contours drawn at levels of $+4\sigma$ (solid) and -4σ (broken) where σ is the root-mean-square density throughout the unit cell.

In summary, the crystallographic analysis shows that the difference in binding constants of the two inhibitors measured by Bartlett and Marlowe (*11*) does not arise from different modes of inhibitor binding and can be attributed to the presence or absence of a specific hydrogen bond.

REFERENCES AND NOTES

1. W. R. Kester and B. W. Matthews, *Biochemistry* **16**, 2506 (1977).
2. A. F. Monzingo and B. W. Matthews, *ibid.* **21**, 3390 (1982).
3. M. A. Holmes and B. W. Matthews, *ibid.* **20**, 6912 (1982).

4. L. H. Weaver, W. R. Kester, B. W. Matthews, *J. Mol. Biol.* **114**, 119 (1977).
5. A. F. Monzingo and B. W. Matthews, *Biochemistry* **23**, 5724 (1984).
6. D. G. Hangauer, A. F. Monzingo, B. W. Matthews, *ibid.*, p. 5730.
7. S. J. Gardell, C. S. Craik, D. Hilverg, M. S. Urdea, W. J. Rutter, *Nature (London)* **317**, 551 (1985).
8. C.-M. Kam, N. Nishino, J. C. Powers, *Biochemistry* **18**, 3032 (1979) (also see references listed therein).
9. D. E. Tronrud *et al.*, *Eur. J. Biochem.* **157**, 261 (1986) (also see references listed therein).
10. P. A. Bartlett and C. K. Marlowe, *Biochemistry* **22**, 4618 (1983).
11. ———, *Science* **235**, 569 (1987).
12. M. F. Schmid *et al.*, *Acta Crystallogr. Sect. A* **37**, 701 (1981).
13. D. E. Tronrud, L. F. TenEyck, B. W. Matthews, *ibid.*, in press.
14. Analysis of the inhibitor ZG^{P}LL will be described in detail elsewhere in connection with the analysis of ZF^{P}LL, another peptide analog that binds in a somewhat different manner.
15. P. A. Bash *et al.*, *Science* **235**, 574 (1987).
16. P. V. Luzzatti, *Acta Crystallogr.* **5**, 802 (1952).
17. M. A. Holmes and B. W. Matthews, *J. Mol. Biol.* **160**, 623 (1982).
18. Figure 4 was generated by P. A. Bartlett and P. A. Bash from the coordinates furnished by B.W.M., using the programs MS (M. Connolly) and UCSF MIDAS at the Computer Graphics Laboratory, University of California, San Francisco (R. Langridge and T. Ferrin).
19. We thank P. A. Bartlett and C. K. Marlowe for the inhibitors and for discussions of the results obtained in Berkeley and in Eugene. We also thank T. Alber for discussions and comments. H.M.H. was supported in part by fellowship DRG-667 of the Damon Runyon–Walter Winchell Cancer Fund. The work was supported in part by grants from the National Science Foundation (PCM8312151), the National Institutes of Health (GM20066), and the M. J. Murdock Charitable Trust.

22 August 1986; accepted 4 December 1986

Calculation of the Relative Change in Binding Free Energy of a Protein-Inhibitor Complex

PAUL A. BASH,* U. CHANDRA SINGH,† FRANK K. BROWN,‡ ROBERT LANGRIDGE, PETER A. KOLLMAN

By means of a thermodynamic perturbation method implemented with molecular dynamics, the relative free energy of binding was calculated for the enzyme thermolysin complexed with a pair of phosphonamidate and phosphonate ester inhibitors. The calculated difference in free energy of binding was 4.21 ± 0.54 kilocalories per mole. This compares well with the experimental value of 4.1 kilocalories per mole. The method is general and can be used to determine a change or "mutation" in any system that can be suitably represented. It is likely to prove useful for protein and drug design.

A NEW METHOD HAS RECENTLY BEEN developed to calculate relative changes in free energy between interacting molecular species. It is based on a thermodynamic perturbation method (*1*) with Monte Carlo (*2*) or molecular dynamics (*3–6*) being used to change or "mutate" one molecule into another. It has been applied to a variety of small molecules to calculate relative changes in free energy of solvation within 1 kcal/mol of experimentally measured values (*2, 5, 6*), and to the conversion of benzamidine to *p*-fluorobenzamidine in trypsin (*7*). The results obtained suggest that the relative free energies of interaction between biological macromolecules and their ligands can be calculated by using a generalization of this perturbation method. We present a computational example to support this belief.

We selected thermolysin for this study because extensive structural and thermodynamic data are available for this protein and its inhibitors (i) Cbz-Gly^P-(NH)-Leu-Leu and (ii) Cbz-Gly^P-(O)-Leu-Leu. X-ray crystal structures of these complexes have been determined (*8*), and binding constants measured (*9*). These constants differ by three orders of magnitude, although the two inhibitors differ only by the replacement of an NH by an O and lead to complexes which are nearly identical [see Fig. 4 in the preceding report (*8*)].

We calculated Gibbs (G) free energy changes according to Eq. 1 (*1*)

$$G(\lambda + d\lambda) - G(\lambda) = -k_B T \ln < \exp\left(-\frac{H(\lambda + d\lambda) - H(\lambda)}{k_B T}\right) >_\lambda \quad (1)$$

where k_B is Boltzmanns' constant, T is the absolute temperature, $<>_\lambda$ indicates the ensemble or time average at intermediate positions along the conversion pathway characterized by the coupling parameter λ, and $H(\lambda)$ and $H(\lambda + d\lambda)$ are the Hamiltonians in the states λ and $\lambda + d\lambda$. In the application below, H is taken to be the interaction energy of the inhibitor with its surroundings. Molecular dynamics with a nonbonded cutoff of 8 Å was used to calculate the time average of the Hamiltonian differences from which ΔG between states A($\lambda = 0$) and B($\lambda = 1$) was evaluated by

$$\Delta G = \sum_{\lambda=0}^{\lambda=1} G(\lambda + \Delta\lambda) - G(\lambda) \quad (2)$$

The characterization of states A and B, and calculation of interaction energies, was done with an empirical force field, using standard AMBER force field values (*10*) except for charges on the inhibitor. Ab initio quantum mechanics, with the STO-3G* basis set, was used to determine electrostatic potential based charges (in atomic units) for both inhibitors (*11*). The main change was at the perturbation site where the amide NH ($q_N = -0.705$, $q_H = 0.227$) group on the leucine attached to the phosphate is converted into an oxygen ($q_O = -0.451$), while the charge on nearby atoms changed by less than 0.1. The ability to transform a system between two such states by using perturbation methods and molecular dynamics has been incorporated into the molecular simulation program AMBER (*12*) in a general way (*13*). Perturbation calculations are carried out by specifying the parameters in the beginning and end states, the number of intervals or "windows" between the states, and the length of time for equilibration and data collection in each window. The program automatically carries out the transformation between the two states during which intermediate energy values for each window are accumulated, stored, and reported. The program and methodology are described in more detail elsewhere (*6*).

Two calculations are required. The first determines the solvation free energy difference between the two inhibitors (ΔG_{solv}), and the second determines the free energy difference in the two inhibitor enzyme complexes (ΔG_{bind}). The difference ($\Delta G_{bind} - \Delta G_{solv}$) is equal to the difference in aqueous solution binding free energies of the two inhibitors, $\Delta\Delta G_{bind}$, which was found by Bartlett and Marlowe (*9*) to be 4.1 kcal/mol.

The phosphonamidate inhibitor, in its x-ray conformation taken from the complex, is placed in a box of 782 waters [Jorgensen TIP3P potential (*14*)] generated by a Monte Carlo simulation, and the system is equilibrated for 4 picoseconds at constant temperature and pressure under periodic boundary conditions (*15*) with SHAKE (*16*) being used to constrain all bond lengths to their equilibrium values. The perturbation is carried out in a series of 20 windows with a $\Delta\lambda = 0.05$. At each λ, 500 steps of equilibration (0.002-picosecond

Department of Pharmaceutical Chemistry, University of California, San Francisco, CA 94143.

*Present address: Chemistry Department, Harvard University, Cambridge, MA 02138.
†Present address: Scripps Clinic and Research Foundation, La Jolla, CA 92037.
‡Present address: Smith Kline and French Laboratories, Philadelphia, PA 19101.